Evaluating Bi-directional Connectionless BLE for Bike-to-Everything Wireless Communications

Pedro Henrique Wo de Alcantara*, Khalil Ben Fredj†, Geert Heijenk‡, Yanqiu Huang†
*University of Twente, pedro.wo@outlook.com
†Pervasive Systems, University of Twente, Enschede, The Netherlands
‡Design and Analysis of Communication Systems, University of Twente, Enschede, The Netherlands
{k.benfredj, geert.heijenk, yanqiu.huang}@utwente.nl

***Abstract*—Bike-to-everything (B2X) communication enhances urban safety by enabling real-time information exchange among bicycles, other road users and infrastructure. A key enabler of B2X is Bluetooth Low Energy (BLE), valued for its low power consumption and widespread adoption. While BLE has been well studied for unidirectional communication, two-way discovery, which requires devices to both advertise and scan to achieve mutual awareness in B2X scenarios, remains largely unexplored. Existing models for bi-directional communication assume ideal channel conditions and lack experimental validation, overlooking real-world factors like radio propagation effects and energy consumption. This makes it unclear whether BLE can support timely and energy-efficient message exchange in realistic environments. To address these gaps, we (i) adapt an existing analytical model to capture hardware-specific BLE behaviors and validate it through targeted real-world experiments; (ii) develop and validate a detailed energy consumption model for two-way communication based on BLE hardware measurements; and (iii) define and empirically evaluate new metrics to assess BLE's reliability and timeliness in realistic non-line-of-sight environments. Our findings offer practical guidance for optimizing BLE configurations in real-world B2X deployments.**

***Index Terms*—B2X, BLE, bi-directional communication.**

I. Introduction

As bicycles become increasingly common in urban environments, interactions between cyclists and other road users introduce new safety challenges. Integrating bicycles into connected traffic systems is therefore essential to improve safety in these mixed environments. Bike-to-everything (B2X) communication offers a promising solution by enabling bicycles to exchange real-time information with nearby vehicles, infrastructure, and other bicycles. This connectivity can significantly enhance situational awareness and help prevent collisions in different traffic scenarios [1].

Among various wireless technologies, Bluetooth Low Energy (BLE) is particularly well-suited for B2X communication due to its low power consumption, widespread adoption in consumer devices, and support for flexible, short-range data exchange. However, many existing studies restrict BLE to unidirectional communication, where some devices act solely as scanners while others function only as advertisers broadcasting information. In such setups, it is critical for the scanning device (e.g., a car or a bicycle) to detect nearby advertisers as quickly as possible to respond promptly to the broadcast information. This process is known as the Neighbor Discovery Process (NDP). Prior works such as [2] and [3] have modeled and optimized NDP to reduce discovery latency. Additionally, studies like [4] and [5] explore energy consumption and performance trade-offs in uni-directional BLE communication, highlighting energy efficiency as essential for practical battery-powered applications.

However, uni-directional BLE communication is limited in practical B2X scenarios that require mutual awareness. In such cases, each device must function as both advertiser and scanner, turning the problem into a two-way discovery process. While the core principles of NDP remain relevant, the process becomes significantly more complex due to BLE's inability to transmit and receive simultaneously. Recent work [6] highlights this challenge, demonstrating that BLE devices experience a *blind time* during which a device cannot scan the channel while actively transmitting. The study evaluates how the blindness effect, under varying BLE parameter settings, influences discovery latency in bi-directional communication scenarios. However, the presented model assumes ideal channel conditions and is validated only through simulations. Moreover, focusing solely on discovery latency overlooks practical challenges, particularly for battery-powered devices where energy consumption is equally critical. In [7], a detailed overview of the energy consumption is modeled for connection-based and connectionless communication. Yet, the impact of BLE parameters on energy cost in bi-directional communication remains unexplored. As a result, it remains unclear whether BLE can support timely and energy-efficient communication in real-world settings. In [8] and [9], the impact of line-of-sight (LOS) and movement in BLE are evaluated with different configurations and with physical experiments. Although these works do not implement the same communication strategy as the B2X system using connectionless BLE, they give interesting insights into how to measure the quality of wireless communications at similar ranges.

To address these gaps, we make three key contributions:

- We adapt the analytical model from [6] and validate it on BLE hardware in two phases: first, through controlled side-by-side tests isolating the impact of blindness; then via line-of-sight tests at varying distances to evaluate the combined impact of blindness and realistic propagation conditions. Our focus is on modeling and measuring mes-

979-8-3503-9281-4/25/$31.00 ©2025 IEEE

sage delivery ratio (MDR), since discovery latency can be analytically derived from MDR [6] and MDR avoids timing inaccuracies common in real-world measurements.
- We develop an energy consumption model offering a comprehensive understanding of how BLE parameters affect energy usage and battery life, and validate it based on hardware measurements.
- We introduce and empirically evaluate novel metrics to assess the feasibility of BLE for timely and reliably message exchange in typical non-line-of-sight (NLOS) environments. Together, these insights enable practical optimization of BLE configurations for real-world B2X applications.

The rest of the paper is organized as follows. Section II introduces background of BLE stack and section III describes our modeling of MDR, energy cost, and novel metrics. The experimentation and results are introduced in section IV, followed by conclusion and future work in section V.

II. Background

BLE operates in the 2.4 GHz band, divided into 40 channels, with channels 37, 38, and 39 reserved for advertising and connection initiation. Once a connection is established, devices assume central or peripheral roles and use the remaining channels for data exchange. BLE can also operate in connectionless mode, where data is embedded in advertising packets and broadcast to any listening device. This mode allows for faster and simultaneous communication with multiple nodes by eliminating the connection setup procedure.

In connectionless BLE, a device operates in one of three states: scan, advertise, or idle as shown in Fig. 1. In the scan mode, the device listens to one of the advertising channels at a time and switches between them in a round-robin manner, with an interval S_i called the scanning interval and a duration per channel defined by the scanning window (S_w). When $S_w < S_i$, the device remains idle in the remaining time of S_i. In the advertising mode, the device transmits N copies of its data across each of the advertising channels, e.g. $N = 2$ in Fig. 1. The advertising window, A_w, controls the delay between transmitted copies. At the generation of data in the application layer, the packets are instantly injected into the Network layer. After a random delay $D_{N2L} \sim \mathcal{U}\{11, 20\}$, N copies of the data are injected in the Link layer. Finally, in between advertising windows a 0-10 ms random back-off link layer delay (D_{LL}) is introduced to avoid synchronized transmissions with other devices and reduce interference [10]. In Table I we summarize the key parameters of BLE.

When nodes act as both advertiser and scanner, a period called *blind time* is created. This can be visualized in Fig. 1 named the blind time zone, when both Node 1 and Node 2 are advertising, making the nodes unable to detect each other. The blind time depends on configurable BLE parameters. It directly affects the message delivery ratio (MDR), i.e., the probability that a message is received. It also affects discovery latency, i.e., the time until the first message is received.

Symbol	Description
S_w	Scanning window duration
S_i	Scanning interval duration
A_w	Advertising window duration
T_{gen}	Message generation period
D_{AdvDur}	Advertising duration
$D_{\text{LL}} \sim \mathcal{U}\{0, 10\}$ ms	Link Layer delay [10]
$D_{\text{N2L}} \sim \mathcal{U}\{11, 20\}$ ms	Network-to-Link Layer injection delay [11]
D_{AdvStart}	Advertising start delay
$D_{\text{Tx/Rx}}$	Mode switch (advertising/scan) delay
I_{scan}	Current during scanning period
I_{Tx}	Current during transmission period
I_{idle}	Current during idle period
N	Number of copies (network count)
$\Phi_{1,2}$	Shift between node 1 and 2 epoch starts
s	State representing the advertising period start

TABLE I: Symbol descriptions used in the analysis.

These effects have been modeled in [6] using a discrete-time analysis that divides time into fixed-length slots and defines an *epoch* as the interval between two message generations. The analysis proceeds in several steps: **(a)** model the advertising duration in each epoch; **(b)** model the start time of the adverting state within each epoch; **(c)** compute the time shift and its probability distribution of two nodes' advertising starting phases by combining the start times and durations. **(d)** determine the MDR by calculating the probability that the time shift results in overlapping transmissions and reception on the same channel, leading to a successful message delivery; **(e)** derive the discovery latency from the MDR; **(f)** generalize the analysis by incorporating the epoch offset $\Phi_{1,2}$ between two nodes, which captures the random time difference in their message generation start times and accounts for all factors influencing their relative timing.

III. Methods

In this section we will first explain the theoretical modeling of message delivery ratio and energy cost as functions of BLE parameters. After that, we introduce the metrics to study whether BLE is feasible for time-critical message exchange in real world environment.

A. Theoretical modeling

We will first explain how we adapt the mathematical model in [6] for MDR. Then we provide the energy cost model to show the parameter tuning options to balance MDR and energy consumption.

1) MDR vs. BLE parameters: Upon initial analysis of the BLE stack implementation on the selected hardware, we observed minor differences in behavior compared to the behavior presented in [6]. Specifically, two key differences were identified: (i) the link layer delay (D_{LL}) is applied prior to the start of each advertising window, rather than following it; and (ii) additional delays occur due to the switching between the advertising and scanning states. It is important to emphasize that these changes stem solely from hardware-specific implementation and only require slight change of the theoretical model proposed in [6].

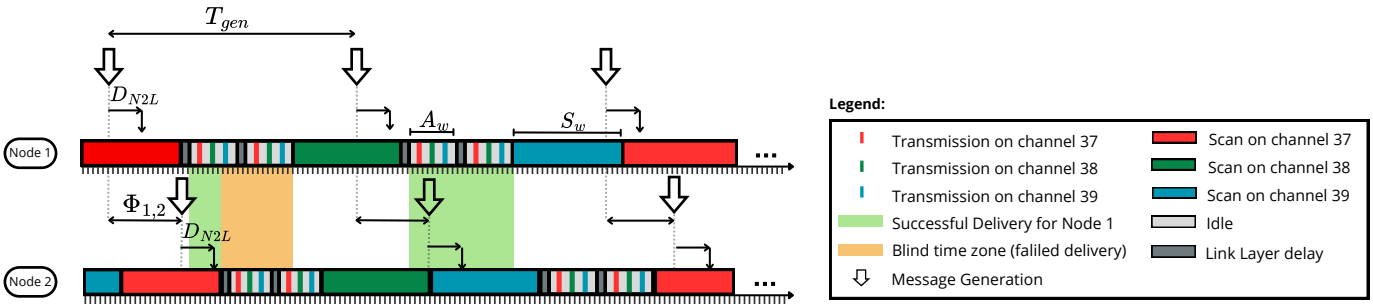

Fig. 1: Bi-directional connectionless BLE communication diagram with two nodes.

Following the analysis in step **(a)** of [6] mentioned in Section II, the duration of the adverting state (D_{AdvDur}) is updated as follows:

$$D_{AdvDur} = 2 \cdot D_{Tx/Rx} + D_{LL,N} + A_{Tx} + \sum_{i=1}^{N-1} (A_w + D_{LL,i}). \quad (1)$$

where $D_{Tx/Rx}$ is the delay that the BLE implementation takes to switch modes, $D_{LL,N}$ and $D_{LL,i}$ are the link layer delays added before each copy transmission, A_{Tx} is the time to transmit into all the advertising channels and A_w is the configured advertising window. Compared to the original model, the variables $D_{Tx/Rx}$, $D_{LL,N}$ and A_{Tx} were added to the formula to better mimic the behavior of the implementation used.

For determining the start of advertising in step **(b)**, we can use:

$$s' \equiv (s + D_{\text{AdvDur}} + k^* \cdot S_w) \pmod{T_{\text{gen}}}. \quad (2)$$

where k^* is the minimum value of ℓ that meets the condition $s + D_{AdvDur} + \ell \cdot S_w \geq T_{gen} + D_{N2L}$. Looking into Eq. (2), we see that the start mainly depends on two factors: the start of the previous epoch and the length of scan windows (S_w). That is because, as shown in Fig. 1, the start depends on how many S_w fit before the next message is generated, the closer the message injection is to the end of a S_w the sooner the message will be sent. Furthermore, we can also calculate the range of possible start times within an epoch with:

$$\begin{aligned} min\{D_{AdvStart}\} &= min\{D_{N2L}\}. \\ max\{D_{AdvStart}\} &= max\{D_{N2L}\} + S_w. \end{aligned} \quad (3)$$

After the above mentioned changes, we can obtain the MDR following step **(c)** and step **(d)** in [6], and further generalize it to different $\Phi_{1,2}$ following step **(f)**. The model shows that by increasing S_w we can enhance the MDR in worst-case scenarios. Such correlation is expected because, as shown in Eq. (3), longer S_w results in a bigger range of possible start times. In fact, as the time gap between message generations of two nodes $\Phi_{1,2}$ decreases, the longer range of the start of the advertising state reduces the probability of nodes synchronization.

2) Energy cost vs. BLE parameters: The energy consumption is important to calculate the battery life of the devices. As shown in [4], the power needed to scan is similar to the power required to transmit packets. However, considering the duration of each phase, their difference becomes more noticeable. That is because scanning is a longer and continuous process, while advertising phases are short peaks of energy followed by idle states where consumption is minimal. To calculate the energy consumption, we analyze all the communication phases within an epoch. Then, the energy cost per epoch, E_{epoch}, is calculated as the sum of the energy consumed during the advertising phase (E_{adv}), the energy consumed during the scan phase (E_{scan}), and the energy consumed to switch modes (E_{switch}):

$$\begin{aligned} E_{adv} &= (D_{AdvDur} - N \cdot A_{Tx} - 2 \cdot D_{Tx/Rx}) \cdot I_{idle} \\ &\quad + N \cdot A_{Tx} \cdot I_{Tx}, \\ E_{scan} &= (T_{gen} - D_{AdvDur}) \cdot I_{scan}, \\ E_{switch} &= 2 \cdot D_{Tx/Rx} \cdot I_{switch}, \\ E_{epoch} &= E_{adv} + E_{scan} + E_{switch}. \end{aligned} \quad (4)$$

There, I_{Tx}, I_{scan}, I_{idle} and I_{switch} are the current consumption during transmission, scanning, idle and mode switch. Additionally, we can estimate the average energy consumption per epoch, $\overline{E_{epoch}}$,with:

$$\begin{aligned} \overline{E_{adv}} &= (\overline{D_{AdvDur}} - N \cdot A_{Tx} - 2 \cdot D_{Tx/Rx}) \cdot I_{idle} \\ &\quad + N \cdot A_{Tx} \cdot I_{Tx}, \\ \overline{E_{scan}} &= (T_{gen} - \overline{D_{AdvDur}}) \cdot I_{scan}, \\ \overline{E_{epoch}} &= \overline{E_{adv}} + \overline{E_{scan}} + E_{switch}. \end{aligned} \quad (5)$$

Here $\overline{D_{AdvDur}}$ is the average duration of the advertising duration, and $\overline{E_{adv}}$ and $\overline{E_{scan}}$ are the average energy cost of the advertising and scanning modes.

The I values are the measured currents on each phase. Multiplying them for the duration of each phase, we get the energy cost per epoch. As we can see, changing the epoch duration and the number of copies transmitted has a direct impact on the energy. That is because they determine how long the node will be actively scanning, advertising or idle.

One way to reduce its cost is by reducing the overall scanning duty cycles (period of active scanning within an epoch divided by the epoch length). Some methods to change the overall duty cycle are: changing the number of copies

sent since the more copies, the longer the device will be in advertising mode; or changing the message generation frequency, as it will modify the epoch length.

In summary, from the above two models, we see that increasing S_w while fixing other parameters can increase MDR without affecting energy consumption, especially with the fact that the energy consumption is mainly defined by the number of copies and the length of the advertising window.

B. Metrics for Physical Feasibility Study

To determine the feasibility of the system in real-world scenarios, we also evaluate other metrics such as the discovery range and the battery life of the system. To analyze the ability to alert users, we define the discovery range as the distance between nodes at the moment of the first received message when two nodes enter the communication range of each other. To determine the success of delivery at each distance, we use the complementary cumulative distribution function (CCDF) to calculate the probability of the first packet being received at a distance greater than X:

$$F(x) = 1 - P(X < x). \tag{6}$$

where X is a random variable representing the distance between nodes at which the first message is received. By evaluating the discovery range we can determine if the system would be able to inform the cyclist of a hazard with enough distance for a maneuver. Further, we compare the maximum achievable message delivery per second (which is the number of generated messages per second) to the actual number of message received per window of one second. This new metric is important to see the effect of channel condition on the message receptions in a mobile scenario where the distance between two bicycles is changing.

Furthermore, we calculate the battery life of the system. This metric is an indicator of how long the system could run before requiring a new recharge of the battery. To estimate the battery life, we use:

$$\text{Battery Life} = \frac{\text{Battery capacity}}{\overline{E_{epoch}}} \cdot T_{gen}. \tag{7}$$

Where $\overline{E_{epoch}}$ is the average energy consumption per epoch, given in Eq. (5).

IV. Implementation & Results

In this section, we will first give an overview of how the BLE and the test setup were implemented. Then we validate the adapted MDR model by the side-by-side test and line-of-sight (LOS) experiments with varying distances, as well as the energy cost model. After that, we evaluate the feasibility of BLE for surrounding awareness applications in typical non-line-of-sight (NLOS) settings using the aforementioned metrics including discovery range, number of updates received per window of time and battery life.

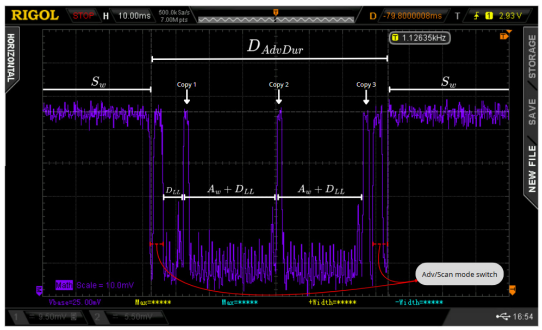

Fig. 2: Oscilloscope screenshot for an epoch.

A. Implementation

To implement the communication setup on a bicycle, we opt for two nRF5340 Development Kit (DK) from Nordic Semiconductors. The DK embeds the nRF5340 System-on-Chip (SoC), which is a popular option for IoT applications using BLE. Regarding hardware, we also used a microSD module (Adafruit's MicroSD card breakout board+) to record packet receptions and an LED for visualization purposes. To synchronize the nodes, we also use IOs for UART communication.

On the software side, our code of the implementation [12] is divided into C scripts representing each module of the system. The scan and the beacon modules are responsible for the BLE-related functions such as scanning and advertising, setting the BLE parameters, simulating the Application layer, and generating messages periodically with a period of T_{gen}.

Regarding the content of the packets, an advertisement payload is restricted to 37 bytes (including flags and identifiers). From those bytes, we have the flexibility to set the Manufacturer's Specific Data Field with a custom structure where we can send the necessary data. Our payload data structure consists of: a packet ID (2 bytes), timestamp (4 bytes), advertising start (2 byte), latitude (4 bytes) and longitude (4 bytes). Since location finding is not part of our scope, the latitude and longitude were implemented as placeholders for future implementations. The remaining data fields were selected to support the test measurements.

To determine the energy cost of communication, we measured the current of the different phases (as shown in Fig. 2) including idle, transmitting, scanning and switching between them with an oscilloscope. We have also validated the duration of each phase compared to our model since it is essential for the estimation of the battery life.

We select different parameter sets (Table II) to assess the impact of the scan window length and the number of copies sent. On one hand, sets 1 and 3 are chosen to compare the effect of changing the number of copies while having the same scan window size. On the other hand, in parameters sets 1 and 2, we assess the effect of changing the scan windows size while having the same number of copies per generated message. We note that we set the advertising window as the smallest allowed value (20ms) as per Bluetooth specifications.

Parameter Set	$S_w(ms)$	$N(copies)$	$T_{gen}(ms)$
1	50	3	200
2	80	3	200
3	50	5	200

TABLE II: Parameter sets used in the tests.

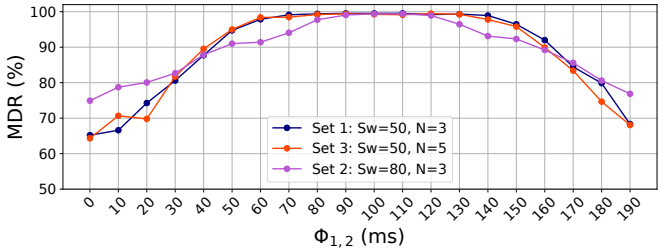

Fig. 3: Message delivery ratio comparison between all parameter sets during side by side test.

In addition to the nRF5340 DKs, we also used an nRF52 DK flashed with Nordic's nRF Sniffer, allowing us to use it as a BLE sniffer, scanning the BLE channels with 100% duty cycle. This serves as a valuable tool for debugging and establishing ground truth, as it eliminates the impact of blind time.

B. Model validation

The side-by-side test is relevant to understand the impact of blind time on the MDR, while removing the effects of channel conditions (due to pathloss and channel fading). The test was done indoors with the two nRF5340 DKs next to each other. Once a test starts, the nodes will generate messages each $200ms$ and will follow the state machine, for 300 seconds, after which a new test is initiated. Each test consists of a fixed shift ($\Phi_{1,2}$) between the generation times of the two nodes. The first test starts with a shift of $\Phi_{1,2} = 0$ and after the completion of each test one node shifts its generation schedule by $10ms$ creating a new shift $\Phi_{1,2} > 0$. The test is completed when all 20 shifts within the $200ms$ generation period are measured.

As shown in Fig. 3, a longer scan window gives better performance with closer synchronization as estimated in the model. This difference is explained by the range of time an advertisement can start within an epoch. In fact, the maximum start time range is increased as we increase S_w, as shown in Eq. (3). With a longer range of possible start times, the chances of each node choosing different start times is increased and, consequently the likelihood of reception is also increased. From Fig. 3, we also see that modifying the number of copies sent does not influence drastically the trend per shift. That is because, as both nodes have the same S_w, they are equally affected by the blind time.

Further, we compared the results with the analytical model in Fig. 4. The model results are similar to the experimental results, having a mean absolute error of 2%, which validates our modified version of the theoretical model. We also notice that the node achieve the best performance with 100 ms shift as the epochs are the most de-synchronized, eliminating the impact of blind time. The model also displays the advantage

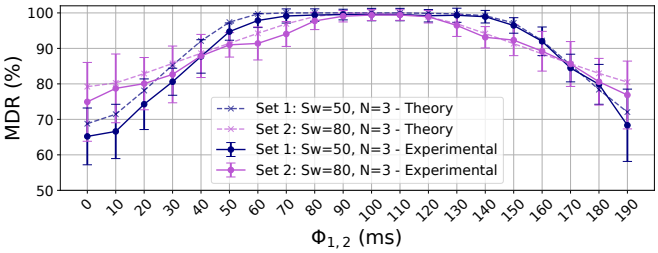

Fig. 4: Comparison between analytical model and experimental data for each parameter set.

of the longer scan window for closer shifts, having a similar behavior throughout the shifts. Looking into the standard deviation bars from the experimental data, we see that the dispersion is higher when the boards are more synchronized. Such behavior occurs because, on those closer shifts, reception is strongly dependent on the randomness of the advertising start time while, when the nodes are fully de-synchronized, any start time would satisfy the reception conditions.

The overall results from the side by side tests show that the model can precisely estimate the impacts of blind time and parameter configuration. As shown Fig. 4, synchronization between nodes has a significant impact on MDR when $\Phi_{1,2}$ is closer to zero. On the other hand, when $\Phi_{1,2}$ gets closer to half of the generation period the best performance is achieved.

Following the side-by-side validation, we conducted line-of-sight experiments at varying distances between BLE boards to assess the combined impact of blindness and realistic propagation effects on MDR. Although these scenarios introduce mild signal attenuation, they enable us to observe how MDR degrades in practice and to evaluate whether the analytical model, which does not explicitly account for range-dependent factors, can accurately capture these performance trends.

We used a similar setup to the side by side test, evaluating different shifts. In this test, the measurements were done outdoors and with the nodes separated by different distances (10, 20, 30, 40, 60, 80 and 100 meters). We also reduced the test duration to one minute per shift. To simulate bicycle conditions, we placed one node in a handlebar bag (one meter from the floor) attached to a bike and the other one at the same height. To achieve LoS conditions, we chose the location of the test as shown in Fig. 5.a which is an open area with no obstructions, and all tests were carried out in a dry weather.

After carrying out the LOS tests, we observe that the distance between nodes does not have a big impact on MDR, and the packet loss is mostly due to blindness effect. To verify this hypothesis, the LOS experiments were repeated using a modified setup in which one of the nodes operated as a sniffer which is continuously scanning without transmitting. This configuration effectively eliminated the blindness effect. The results showed a message delivery rate of approximately 99% at the sniffer, confirming that the majority of packet loss observed in the standard two-node configuration comes from the blindness effect and barely from the inter-node distance.

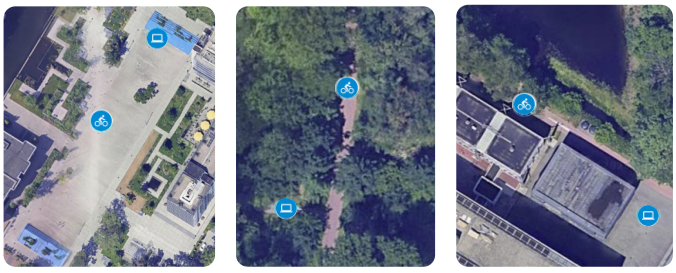

(a) LOS test (b) NLOS test - vegetation (c) NLOS test - buildings

Fig. 5: Satellite view of the test locations. The computer and bike icons represent the nodes position. For the NLOS test, the bike icon is the moving node while the computer icon is the static node

Further, we performed the oscilloscope measurements to validate the energy model. We identified that the current increases in 3 activities: during scanning, during packet transmission, and during mode switch. Those sections (I_{scan}, I_{Tx} and I_{switch}) have an average current of 7 mA while the idle (I_{idle}) sections have an average of 2.5 mA. Furthermore, we observed that the transmission duration (A_{Tx}) in all channels takes approximately 1.3 ms, and the mode switch ($D_{Tx/Rx}$) takes 4 ms. Table III shows an instance of the observed energy consumption in an epoch.

Phase	Duration (ms)	Energy cost (10^{-6} mAh)
Mode switch (high phase)	3.4	6.6
Mode switch (low phase)	0.6	0.4
Copy transmission	1.3	2.5
Idle ($N = 3$)	52.3	36.3
Idle ($N = 5$)	99.7	69.2
Scanning ($N = 3$)	137	266.3
Scanning ($N = 5$)	87	169.1

TABLE III: Energy consumption in a single epoch

C. Feasibility test

In this batch of tests, our goal is to evaluate whether BLE is feasible for timely and reliably message exchange in typical non-line-of-sight (NLOS) environments. The measurement strategy was to have a moving bike approaching an intersection (at a constant speed of 25 km/h) and a static bike at a (visually) blind spot. The tests were done in two locations, where the main difference is that LoS was blocked by vegetation or buildings (Fig. 5b and 5c). We considered the receptions within a 100 m range as it gives the rider enough time to react. Additionally, we used an action camera to record both an LED that blinked whenever a packet was received, and the floor, where we marked the distance from the intersection. Later, we analyze the footage to identify the bike position when the first message was received within the 100 m range.

Regarding the parameter settings, we tested the same parameters as in Table II. To account for the worst-case scenario of shifts, we only tested the case where the message generations are fully synchronized between both nodes ($\Phi_{1,2} = 0$).

After 20 repetitions for each location and set, we get the CCDF of the distance at which each node received the first

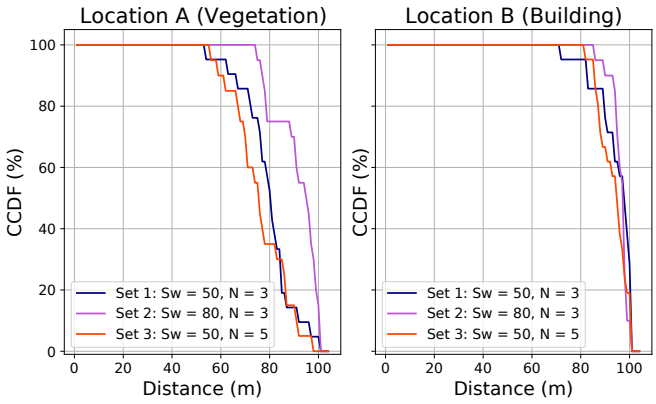

Fig. 6: CCDF of the distance from the intersection for the first received message.

message when approaching each other. In Fig. 6, we see that the configuration with $S_w = 80ms$ showed better performance compared to the ones with scan windows of $S_w = 50ms$. That is explained by the advantage of longer S_w values on closer synchronization. Also, in the vegetation scenario, the parameter sets with different number of copies but with the same scan windows show similar performance. This latter result aligns with the observation on Fig. 3 where fixing the scan window while changing the number of copies does not have a big effect on the communication performance. We can observe that vegetation affected reception more strongly than the building. The dense leaves along the path reduced signal strength. In contrast, the building's metallic structure aided propagation through reflections and multipath effects.

Later, we analyzed the packet arrivals in the moving bike. Fig. 7 gives an in-depth view of reception as the bikes approach each other by showing the average number of messages per window duration of one second from the intersection. There, we can see that set 2 receives messages earlier and in larger amounts than the other sets, and that all sets receive messages even before the comfort zone. As defined in [13], the comfort zone is the time before reaching an obstacle where the cyclist can comfortably maneuver or break to avoid collision. Further, we observe that the number of detected messages increases as the nodes get closer, that is a result of the improved signal strength. We should keep in mind that, as $T_{gen} = 200ms$, the maximum number of packets that can be sent per second is 5, not including copies. It is also relevant to point out that set 2 showed a detection range further than 100 m in some tests, but since we chose a range of 100 m, only packets received in this range were considered.

In summary, the Non-LoS tests helped us identify two key behaviors. First, larger scan windows show a significant advantage over shorter windows in worse-case conditions ($\Phi_{1,2} = 0$). Second, sets 1 and 3 showed very similar results due to the common S_w, meaning that tuning the number of copies is a possible method for energy optimization without major impact on communication quality. Furthermore, observ-

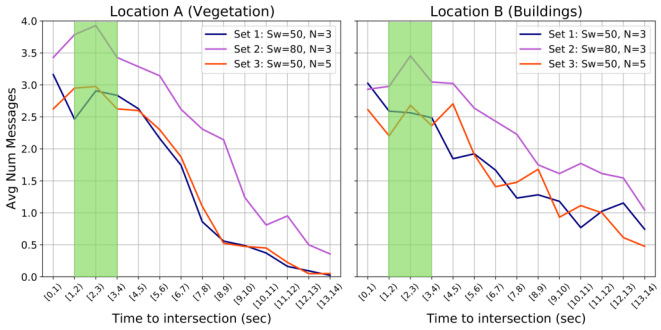

Fig. 7: Average packets per window of one second to the intersection and comfort zone for maneuvering (in green) based on [13].

ing the discovery range, the results demonstrate that B2B wireless communication, under the tested conditions, could allow real-time surrounding awareness, with a first reception that allows for comfortable maneuver. Moreover, comparing test locations, we see that the type of obstruction (vegetation or buildings) also impacts the performance of the system.

In Table IV, we show an estimation of battery life when using a 150 mAh coin battery. As shown, with any of the parameter sets tested, the system would comfortably have a full day of continuous use before requiring to be charged. Besides that, we see the impact of parameter tuning on energy consumption. Increasing the advertising phase via the number of transmitted copies is a viable way to change energy use. On the other hand, changing the scan window has no major impact on the consumption per epoch. Compared with previous results showing that sets 1 and 3 have the same performance, increasing the number of copies transmitted is a viable way to decrease consumption without compromising performance.

N	Epochs	Cost per epoch (10^{-6} mAh)	Battery life
3	464,396	323.2	25.8 h
5	568,181	264.1	31.5 h

TABLE IV: Overall battery life estimation based on energy consumption

V. Conclusion & Future Work

This paper provides a practical evaluation of bi-directional BLE communication performance in B2X scenarios. Building on prior analytical models, we expand the understanding of BLE behavior through real-world experiments, focusing on its effects on message delivery ratio and energy consumption. Our results, supported by novel metrics, demonstrate significant potential for BLE to support reliable and efficient B2X communication. Under the tested scenarios, the minimum requirements for time-critical applications are met, and packets can reliably carry meaningful information to enhance cyclist safety. In particular, the scan window and number of message copies emerged as critical tunable parameters: increasing the scan window notably improves MDR under worst-case synchronization, while increasing the number of copies can extend battery life by approximately six hours without compromising reception.

While these findings are encouraging, further research is needed to refine and optimize BLE configurations under more challenging conditions. Future work should evaluate performance in busier wireless environments with interference and packet collisions, and develop systematic methods to balance energy efficiency and communication reliability. With these enhancements, BLE communication holds strong potential to become a key enabler of safer and more connected urban traffic systems.

References

[1] J. C. García-Ortiz, J. Silvestre-Blanes, and V. Sempere-Payá, "Experimental Application of Bluetooth Low Energy Connectionless in Smart Cities," *Electronics 2021, Vol. 10, Page 2735*, 2021.

[2] G. Shan and B.-h. Roh, "Performance model for advanced neighbor discovery process in bluetooth low energy 5.0-enabled internet of things networks," *IEEE Transactions on Industrial Electronics*, vol. 67, no. 12, pp. 10 965–10 974, 2020.

[3] P. H. Kindt, S. Narayanaswamy, M. Saur, and S. Chakraborty, "Optimizing ble-like neighbor discovery," *IEEE Transactions on Mobile Computing*, vol. 21, no. 5, pp. 1779–1797, 2022.

[4] B. Luo, J. Gao, and Z. Sun, "Energy modeling of neighbor discovery in bluetooth low energy networks," *Sensors*, vol. 19, no. 22, 2019. [Online]. Available: https://www.mdpi.com/1424-8220/19/22/4997

[5] C. Gomez, J. Oller, and J. Paradells, "Overview and evaluation of bluetooth low energy: An emerging low-power wireless technology," *Sensors*, vol. 12, no. 9, pp. 11 734–11 753, 2012. [Online]. Available: https://www.mdpi.com/1424-8220/12/9/11734

[6] K. Ben Fredj, G. Heijenk, and Y. Huang, "Modeling of mutual connectionless ble discovery in the context of b2x communications," in *IEEE Vehicular Networking Conference*, 2025, 16th IEEE Vehicular Networking Conference, VNC 2025, VNC 2025 ; Conference date: 02-06-2025 Through 04-06-2025. [Online]. Available: https://vnc2025.ieee-vnc.org/

[7] P. H. Kindt, D. Yunge, R. Diemer, and S. Chakraborty, "Energy modeling for the bluetooth low energy protocol," *ACM Transactions on Embedded Computing Systems (TECS)*, vol. 19, no. 2, pp. 1–32, 2020.

[8] H. Karvonen, C. Pomalaza-Ráez, K. Mikhaylov, M. Hämäläinen, and J. Iinatti, "Experimental performance evaluation of ble 4 versus ble 5 in indoors and outdoors scenarios," in *Advances in Body Area Networks I: Post-Conference Proceedings of BodyNets 2017*. Springer, 2018, pp. 235–251.

[9] J. C. García-Ortiz, J. Silvestre-Blanes, and V. Sempere-Payá, "Experimental application of bluetooth low energy connectionless in smart cities," *Electronics*, vol. 10, no. 22, 2021. [Online]. Available: https://www.mdpi.com/2079-9292/10/22/2735

[10] "Link layer specification," accessed: 04-06-2025. [Online]. Available: https://www.bluetooth.com/wp-content/uploads/Files/Specification/HTML/Core-54/out/en/low-energy-controller/link-layer-specification.html

[11] "Mesh profile," Jan. 2019, accessed: 04-06-2025. [Online]. Available: https://www.bluetooth.com/specifications/specs/mesh-profile-1-0-1/

[12] PedroBR13, "BLE_for_B2X: Bike-to-bike communication via ble," https://github.com/PedroBR13/BLE_for_B2X, 2025, accessed: 2025-08-08.

[13] O. Lee, A. Rasch, A. L. Schwab, and M. Dozza, "Modelling cyclists' comfort zones from obstacle avoidance manoeuvres," *Accident Analysis Prevention*, vol. 144, p. 105609, 2020. [Online]. Available: https://www.sciencedirect.com/science/article/pii/S0001457519317294